*International Journal of Innovative Computing, Information and Control*
Volume **8**, Number **3(A)**, March **2012**

ICIC International ©2012 ISSN 1349-4198
pp. 1787–1798

# MULTI-SCALE BASED UNIFIED MODELING AND SIMULATION OF PART SURFACE TOPOGRAPHY

Chan Qiu, Zhenyu Liu*, Jianrong Tan and Wanghui Bu

State Key Laboratory of CAD and CG
Zhejiang University
No. 866, Yuhangtang Rd., Hangzhou 310058, P. R. China
{qc; egi; buwanghui}@zju.edu.cn; *Corresponding author: liuzy@zju.edu.cn

Received November 2010; revised April 2011

Abstract. *This paper concentrates on the multi-scale based unified modeling method of part surface topography. First of all, a three-dimensional multi-fractal characteristic function is proposed, which can be used to describe the micro-topography of a three-dimensional multi-fractal rough surface. The altitude variation of surface topography can be regarded as a series of stochastic signals, so the multi-scale information can be extracted by wavelet analysis and decomposed into four scales. The extracted multi-scale redundant information is optimized into multi-resolution information. Then, a method is proposed to evaluate the consistency of the multi-scale information, and the information transmission model of multi-scale part surface is also built. Finally, the method of multi-scale modeling is verified to be feasible by multi-performance simulation of the gem processing machine tool.*
**Keywords:** Multi-scale, Multi-resolution, Multi-fractal, Wavelet analysis

1. **Introduction.** The quality of part surface has been a key factor in product multi-performance simulation. Because mechanical part surfaces cannot be smooth planes actually, the geometrical error has quite an effect on product performance. When two surfaces of a kinematic pair contact each other, the contact objects are micro-bulges of the two surfaces actually. As the part moves, elastic-plastic deformation and shear failure occur on those micro-bulges, and the product wear-resistant quality is affected. Due to the small radius of curvature, stress concentration can be caused easily in the valley bottom between the micro-bulges, and it brings fatigue crack, so that the product fatigue-resistant quality is also affected. Moreover, as to clearance fit and interference fit, surface geometrical error may cause the change of fit property.

It has been discovered that the phenomenon of multi-scale exists in product multi-performance simulation. One part surface is concerned always with detail information of different scales in different kinds of simulations and analyses. In frictional and wear analysis, the model of micro-scale is needed, since the real contact area between two surfaces depends on the short wave component of rough surfaces. In product assembly and maintenance simulations, it is concerned that whether the macro geometrical error that is made up of long wave component affects the product assembly performance. Moreover, the kinematic accuracy of a part is restricted by medium wave component of rough surfaces. Part surface topography can be treated as superimposition of roughness, waviness and form error, where roughness belongs to the geometrical error of micro-scale; waviness belongs to the geometrical error between micro-scale and macro-scale; form error belongs to the geometrical error of macro-scale.

Dobrzanski and Pawlus [1] separated surface roughness and waviness by Gaussian convolution, Gaussian regression and spline filters and compared the performances of these methods. Wilson et al. [2] converted the topography of roughness into superimposed sine waves at different scales by Fourier transformation and proposed a multi-scale surface separation model which can make predictions for the real contact area and the contact resistance. Grzesik and Brol [3] extracted surface roughness from different workpiece materials after finish turning by continuous wavelet transform of Morlet and 'Mexican hat' and detected the fractal properties of the roughness profile. Zhang et al. [4] measured a two-dimensional real engineering surface and extracted mean line and roughness in frequency domain using a filter constructed by combining B-spline with variance difference. Chen and Li [5] measured the profile line and the profile surface of an actual workpiece, and found a reference line and a reference surface for roughness evaluation by wavelet analysis, so roughness could be separated from other components of the surface. Lu and Li [6] simulated engineering surfaces by W-M function and proposed a composite surface assessment method based on wavelet to identify and analyze composite surface characteristics at different scales. Hu [7] proposed a surface error reconstitution method based on discrete wavelet analysis, and assessed the mean line of surface roughness, and then built a filtering model for separating surface errors.

At present, most researches on part surface topography are based on independent scales. Although all the researchers above extracted related information from rough surfaces, since there are different expressions to the models of part surface topography at different scales, it is hard to associate surface topographies at different scales, build the unified multi-scale model and carry out further researches and analyses based on the multi-scale model. Meanwhile, in simulations at different scales, the geometric models and the computation models were usually simplified due to the restriction of computational complexity, modeling time and cost, etc. Moreover, the micro-topography of rough surface was simulated only by two-dimensional curves, and there were very few researches studied in three-dimensional environment.

In this paper, the multi-scale based unified modeling method of part surface topography is proposed. Three-dimensional multi-fractal rough surface is simulated by multi-fractal characteristic function defined in this paper, and the altitude information is decomposed afterwards by wavelet analysis into four scales. Then, the methods of multi-resolution optimization and consistency evaluation are proposed, which can ensure the least loss of details at each scale. Finally, the process of information transmission and coupling in the life cycle of part surface is studied. The multi-scale model of part surface topography uses the unified expression to describe the topography of part surface at different scales, and the association of surface topography between macro-scale and micro-scale is established. The surface models of different scales are applied to different performance simulations, and the storage efficiency and computational efficiency are improved.

## 2. Expression and Simulation of the Micro-Topography of Three-Dimensional Multi-Fractal Rough Surface.

In order to build the multi-scale model of part surface topography, firstly the micro-topography of rough surface should be simulated in computer. Because the altitude variation of mechanical part surface topography is a non-stationary stochastic process with the characteristic of multi-scale, we can consider that it is continuous, non-differentiable and statistically self-affine [8,9]. By conventional methods, it is difficult to describe the micro-topography of a rough surface with the characteristics mentioned above, while fractal theory has the superiority to describe the micro-topography of part surface at all scales without the restraint of resolution and sample length.

Ausloos and Berman described the three-dimensional stochastic process in polar coordinate system by introducing multiple variables to the two-dimensional Weierstrass-Mandelbrot (W-M) function [10,11]. High precise surfaces machined by milling, grinding or turning have the characteristics of multi-fractal and isotropy, and these characteristics are related to the surface processing condition and the surface roughness class [12-14]. Therefore, using the micro-topography of multi-fractal surface will meet the practical situation of mechanical parts and improve the authenticity of product multi-performance simulation afterwards. This work generalizes the A-B functions in rectangular coordinate system, so that the micro-topography of three-dimensional multi-fractal rough surface can be simulated. Regarding multi-fractal part surface, there are various fractal dimension $D$ and fractal roughness $G$ in various spectrum regions, so the multi-fractal surface can be described separately by independent parameters in each spectrum region. The three-dimensional multi-fractal characteristic function is defined as:

$$\begin{aligned} z(x,y) = \; & L\left[\frac{\ln\gamma}{M}\right]^{\frac{1}{2}} \sum_{i=1}^{i_{\max}} \left[\frac{G_i}{L}\right]^{(D_i-2)} \sum_{m=1}^{M} \sum_{n=n_i}^{n_{i+1}} \gamma^{(D_i-3)n} \\ & \cdot \left\{ \cos\phi_{m,n} - \cos\left[ \frac{2\pi\gamma^n (x^2+y^2)^{\frac{1}{2}}}{L} \cos\left[ \tan^{-1}\left(\frac{y}{x}\right) - \frac{\pi m}{M} \right] + \phi_{m,n} \right] \right\} \end{aligned} \tag{1}$$

where $x$ and $y$ are rectangular coordinate values of any point on the rough surface; result $z$ is the altitude value of this point; $D_i$ $(2 < D_i < 3)$ and $G_i$ represent the corresponding fractal dimension and fractal roughness in each spectrum region; $i_{\max}$ is the number of multi-fractal; $L$ is the sampling length; $\gamma$ $(\gamma > 1)$ is a scale parameter which controls the density of frequencies of the rough surface; $M$ denotes the number of superposed ridges; $n$ is the times of summation and $n_{\max} = \text{int}\left[\dfrac{\log(L/L_s)}{\log\gamma}\right]$, where the bracket means rounding operation; $L_s$ is the cut-off length decided by the resolution of measuring device; $\phi_{m,n}$ is a stochastic phase in the interval $[0, 2\pi]$.

## 3. Division, Extraction and Optimization of the Multi-Scale Information of Part Surface Topography.

3.1. **The criterion of dividing part surface into different scales.** The altitude variation of three-dimensional surface topography can be regarded as a series of stochastic signals, and passes three filters which have the same transmission characteristics but different cut-off lengths, so that the surface characteristics can be separated into different scales, and more information can be provided at each scale. According to GB/T 3505-2000, the practical profile is the result of applying short wave filter $\lambda_s$, and the roughness profile is the result of keeping on applying filter $\lambda_c$ to the practical profile. The waviness profile is the result of applying filters $\lambda_s$ and $\lambda_c$ successively to the practical profile, while form error is the profile of applying short wave filter $\lambda_f$ to the practical profile. The sketch is shown in Figure 1.

3.2. **Multi-scale information extraction based on wavelet analysis.** A stationary signal can be decomposed into a series of superimposed sine waves by Fourier transform. Regarding a non-stationary signal such as altitude variation of rough surface, it needs to be decomposed into superimposed wavelets by wavelet analysis. The essence of wavelet analysis is a process of filtering, whose time window and frequency window can be both changed, and has been applied successfully in image processing [15-17] and sound processing [18,19]. In this paper, the altitude information of a stochastic three-dimensional

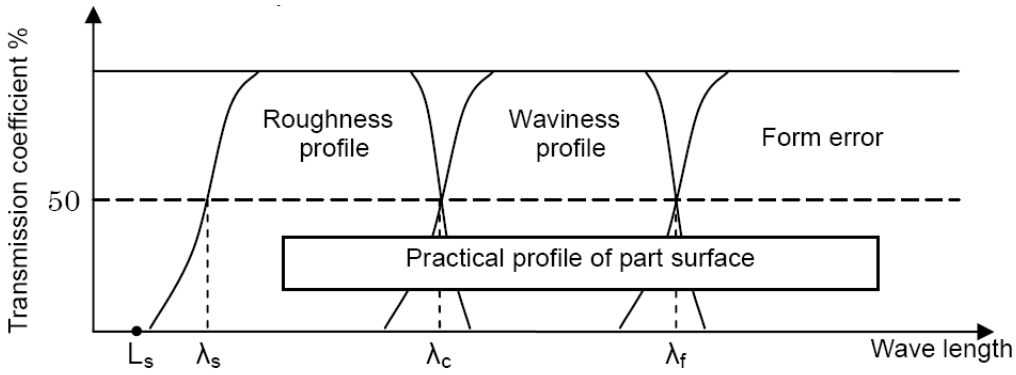


FIGURE 1. Division of different wave lengths of part surface

rough surface is decomposed by wavelet analysis into four scales, so that various kinds of errors can be extracted at various scales.

The altitude data of the three-dimensional multi-scale surface is transformed into two-dimensional Part Surface Altitude Field (PSAF), and two-dimensional discrete wavelet analysis is carried out by using Mallat decomposition and restructing algorithm, which has both row transformation and column transformation and decomposes low frequency component (approximate signal) in every step. The rows of PSAF $C_{j+1} = \{C_{j+1,k,m}\}_{k,m}$ passes the low-pass filter $\{\bar{h}_{-k}\}_{k\in Z}$ and the high-pass filter $\{\bar{g}_{-k}\}_{k\in Z}$, and the outputs of the two filters are sampled with even number, so that the PSAF is divided into two parts, whose left is the low-frequency sub-band, and right is the high-frequency sub-band. Then the columns of each sub-band pass two filters separately, so that the low-frequency sub-band $C_j$, the high-frequency sub-band $D_j^1$ in horizontal direction, the high-frequency sub-band $D_j^2$ in perpendicular direction and the high-frequency sub-band $D_j^3$ in diagonal direction are obtained. Now the row resolution and the column resolution are half of that of original signal, and the size of each sub-band is quarter of that of original signal. The low-frequency sub-band $C_j$ can be decomposed further into $C_{j-1}$, $D_{j-1}^1$, $D_{j-1}^2$ and $D_{j-1}^3$. Figure 2 shows the process of decomposition, where $H$ means high-pass filtering, $L$ means low-pass filtering, the area of $LL$ retains the approximate information of PSAF, and the areas of $HL$, $LH$ and $LL$ remain the high-frequency information of Part Surface Altitude Filed in horizontal, vertical and diagonal directions. The Mallat restructing algorithm is realized by interposing zero between two adjacent values of the approximate signal and the high-frequency detail signals, and passing the low-pass filter $\{h_{-k}\}_{k\in Z}$ and the high-pass filter $\{g_{-k}\}_{k\in Z}$ in the row direction and the column direction separately, and finally summing the four outputs.

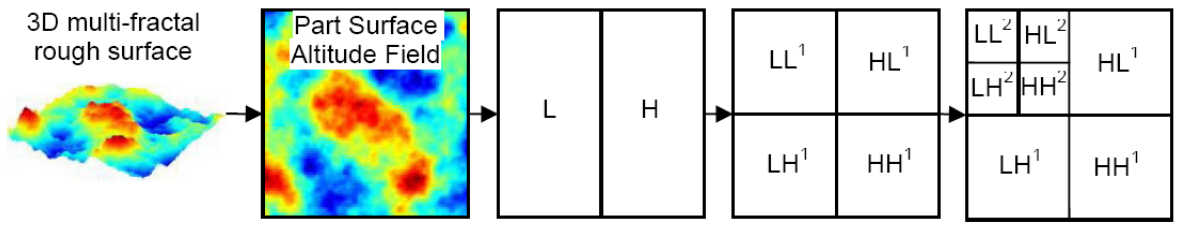


FIGURE 2. Sketch of wavelet decomposition of three-dimensional multi-fractal surface

3.3. **Multi-resolution optimization of the multi-scale information.** The surface altitude information of the four scales, which is obtained by means of wavelet decomposition and reconstruction of part surface topography, has the same resolution actually. Because the curvature variation ranges of surfaces are very different at various scales, it will certainly cause data redundancy by describing the multi-scale information with the same resolution, and decrease storage efficiency and computational efficiency of the whole system. So this work will take multi-resolution optimization of the multi-scale information, and use various resolutions to describe surface altitude information at various scales.

According to Nyquist sampling theorem, the sampling frequency should be at least twice the highest frequency contained in the signal, that is $f_s \geq 2f_{\max}$, and the digital signal will preserve the whole information of original signal after sampling. Three rules of multi-resolution optimization based on Nyquist sampling theorem are proposed in this paper, which are defined as follows:

**Rule 3.1.** *Regard three-dimensional part surface as a two-dimensional altitude signal, and simulate the process of sampling the continuous signal by means of generating discrete points on the multi-fractal surface. In order to obtain the whole required information of the multi-scale model, the original cut-off length which is used to generate multi-fractal surface should be* $L_s \leq \lambda_s/2$, *and the original number of sampling points is* $n_0 = (L/L_s)^2$.

**Rule 3.2.** *Transform the surface of form error into two-dimensional PSAF, and simulate the process of multi-resolution optimization by means of sampling the surface of form error. Let the optimized sampling step length of form error be* $L_{form} = \lambda_f/2$, *and the whole information contained in form error will be preserved.*

**Rule 3.3.** *The optimized sampling step length of the roughness profile and the waviness profile can be obtained likewise. Because the practical profile contains the information of roughness, waviness and form error, its optimized sampling step length equals that of the roughness profile, which has the shortest wave length in the multi-scale model.*

On the basis of the rules mentioned above, the multi-resolution optimized coefficient matrix of multi-scale information of part surface topography is defined as follows:

$$\mathrm{A}_{multi} = \begin{bmatrix} \alpha_{roughness} \\ \alpha_{waviness} \\ \alpha_{form} \\ \alpha_{practical} \end{bmatrix} = L_s^2 \begin{bmatrix} (1/L_{roughness})^2 \\ (1/L_{waviness})^2 \\ (1/L_{form})^2 \\ (1/L_{practical})^2 \end{bmatrix} = 4L_s^2 \begin{bmatrix} 1/\lambda_s^2 \\ 1/\lambda_c^2 \\ 1/\lambda_f^2 \\ 1/\lambda_s^2 \end{bmatrix} \tag{2}$$

and after multi-resolution optimization the number of sampling points of the multi-scale model of part surface topography is reduced to

$$N_{multi} = n_0 \cdot A_{multi} \tag{3}$$

## 4. The Consistency Evaluation and the Information Transmission Model of Multi-Scale Part Surface.

4.1. **The consistency evaluation of part surface based on mutual information.** Before simulation and verification using the multi-scale model separated from part surface by wavelet analysis, it is necessary to ensure the information consistency between the multi-scale model and the practical profile. In this paper, the innovative concept of Mutual Information (MI) is introduced into the measurement of the consistency between two stochastic surface profiles. It shows the common information of two stochastic surfaces, and indicates the relevance between two surfaces. According to Shannon information theory, the information entropy is the mathematical expectation of self-information, which

represents average information of a stochastic surface. The information entropy of part surface $X$ is defined as follows:

$$H(X) = -\sum_{i} P_X(x_i) \cdot \log P_X(x_i) \tag{4}$$

where $x_i$ is the altitude value of PSAF; $P_X(x_i)$ is the marginal probability distribution of altitude. Joint entropy is the total information of two stochastic surfaces. The joint entropy of part surface $X$ and part surface $Y$ is defined as follows:

$$H(X,Y) = -\sum_{j}\sum_{i} P_{X,Y}(x_i, y_i) \cdot \log P_{X,Y}(x_i, y_i) \tag{5}$$

where $P_{X,Y}(x_i, y_i)$ is the joint probability distribution. MI is expressed by the information entropy and the joint entropy of the two part surfaces:

$$MI(X,Y) = \sum_{j}\sum_{i} P_{X,Y}(x_i, y_i) \cdot \log \frac{P_{X,Y}(x_i, y_i)}{P_X(x_i) \cdot P_Y(y_i)} = H(X) + H(Y) - H(X,Y) \tag{6}$$

The more common information the two surfaces contain, the smaller is the joint entropy, and the larger is the MI. For the purpose of improvement of the robustness in the consistency evaluation of part surface, Normalized Mutual Information (NMI) is improved in this paper, which was used in the medical image alignment [20]. Restrain MI and the joint entropy of two surfaces mutually, and the maximum value is limited to 1. Part Surfaces Mutual Information ($PSMI$) is proposed in this paper and defined as follows:

$$PSMI(X,Y) = \frac{H(X) + H(Y)}{H(X,Y)} - 1 = \frac{MI(X,Y)}{H(X,Y)} \tag{7}$$

If and only if two part surfaces are just the same, $PSMI$ reaches the maximum value, $PSMI_{\max} = 1$. The $PSMI$ of the roughness profile, the waviness profile and the form error profile towards the practical profile are denoted by $PSMI_{roughness}$, $PSMI_{waviness}$, $PSMI_{form}$, and the total $PSMI$ of the multi-scale model of part surface topography is:

$$PSMI_{multi} = PSMI_{roughness} + PSMI_{waviness} + PSMI_{form} \tag{8}$$

The larger $PSMI_{multi}$ is, the more common information is contained between the multi-scale model of part surface topography and the practical profile, and the better is the consistency of the multi-scale model towards the practical profile.

4.2. **Information transmission and coupling of multi-scale part surface.** A large amount of information has been generated during creation, extraction, analysis and application of the multi-scale part surface, and should be transmitted and coupled to each other in the life cycle of part surface. The information transmission model of multi-scale part surface is shown in Figure 3.

Fractal surface information includes physical attributes and fractal parameters, which are used to generate the altitude values of multi-fractal surface. Fractal parameters can be adjusted at any time when it is necessary, and a new rough surface will be created instantly which is mapped to the key part of product virtual prototype afterwards, then the information in the multi-scale model will be updated synchronously. Wavelet analysis information includes the key parameters, which are used to extract multi-scale information from multi-fractal surface, and these parameters are usually invariable during the whole process of surface information transmission.

Multi-scale information of roughness, waviness, form error and practical profile is obtained after wavelet analysis. The consistency of the three formers is evaluated towards the practical profile, and they can be also superimposed at different scales in order to

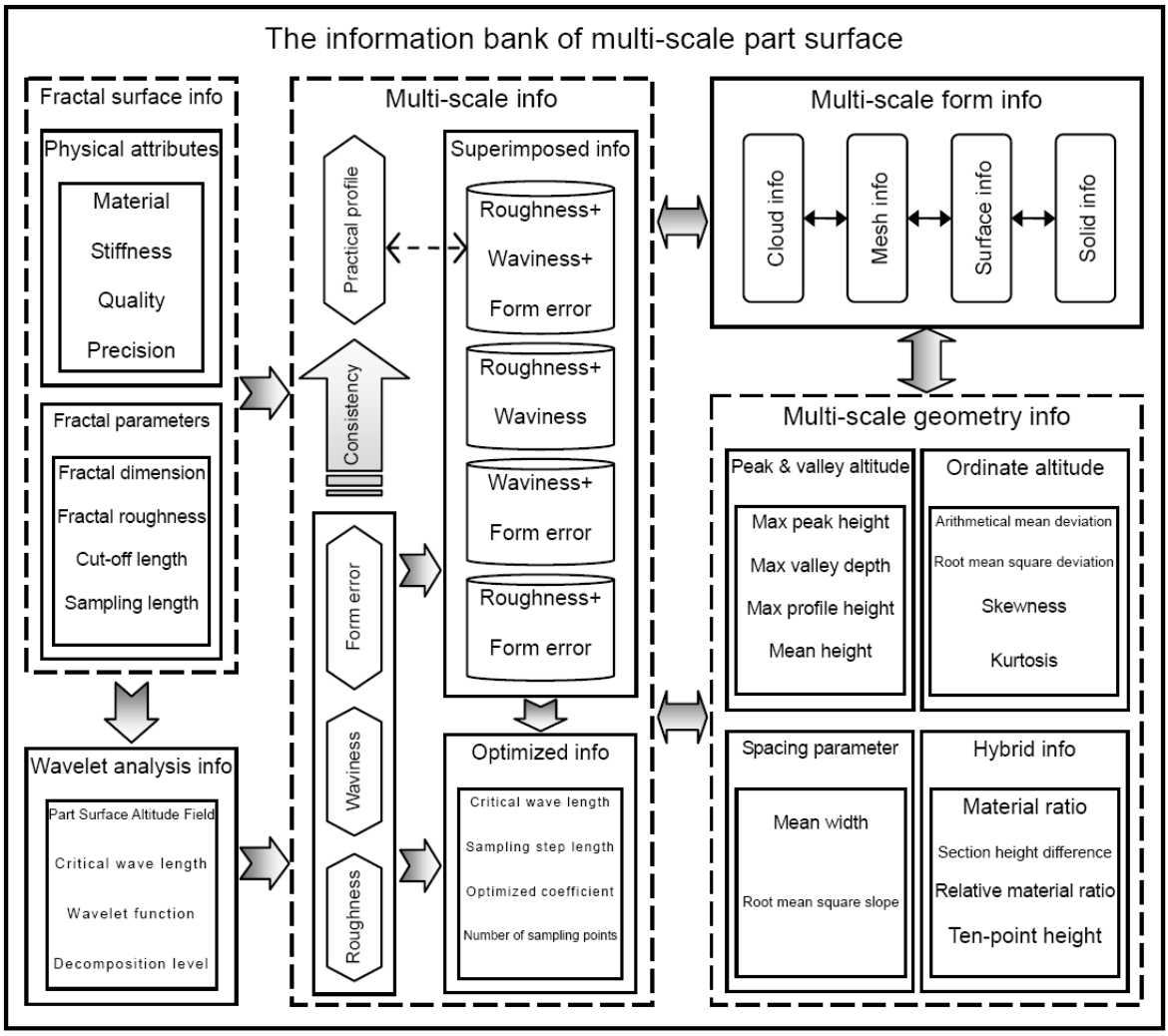


FIGURE 3. Information transmission model of multi-scale part surface

meet the demands of various applications. It must be pointed out that the maximal error between each sampling point of the superimposed profile and the practical profile reaches $10^{-16}$ order of magnitude, and it is calculated that the value of their *PSMI* is 1, so they can be considered as equivalent profiles. Multi-resolution optimized information includes some parameters used to optimize the four profiles and the four superimposed profiles.

Multi-scale form information, which is obtained by importing the optimized multi-scale information of part surface into CAD systems, includes the information of point cloud models, mesh models, surface models and solid models of all scales, and they are also transmitted to each other. Multi-scale geometry information, which is obtained by analyzing the multi-scale form information further, describes the parameters used to express the relationship between the peaks and the valleys of the rough surface profile, the parameters defined by the ordinate mean value, the parameters defined by the profile element width, and other related parameters.

## 5. **Simulation Results.**

5.1. **The building of the multi-scale geometric model of a part surface topography.** The case of multi-scale modeling in this paper is the guide rail of the gem processing machine tool, as shown in Figure 4. The 5mm×5mm area of the guide rail is sampled,

and the three-dimensional multi-fractal rough surface is created according to Equation (1). The parameters which are used to generate the multi-fractal rough surface are listed in Table 1, and the surface topography is plotted as shown in Figure 5.

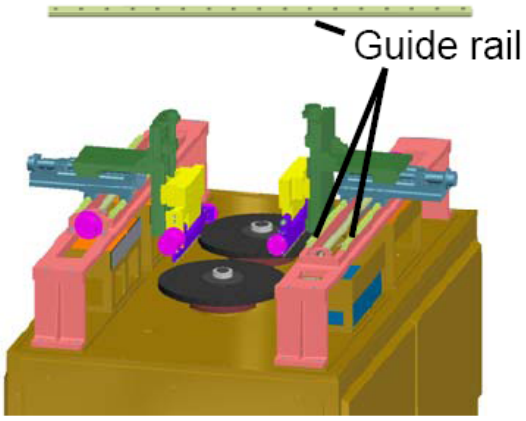


FIGURE 4. Virtual prototype of the gem processing machine tool and its guide rail

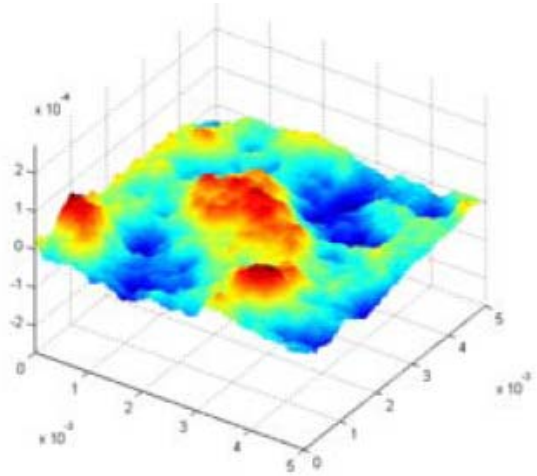

FIGURE 5. Simulation of multi-fractal rough surface topography

TABLE 1. Parameters about the three-dimensional multi-fractal rough surface

| Number of multi-fractal $i$ | Fractal dimension $D_i$ | Fractal roughness $G_i$/m | Stochastic phase in this case $\phi_i$/rad | Sampling length $L$/m | Cut-off length $L_s$/m | Scale parameter $\gamma$ | Number of superposed ridges $M$ | Times of summation $n_{\max}$ |
|---|---|---|---|---|---|---|---|---|
| 1 | 2.25 | $3.36\times10^{-11}$ | $0.64\pi$ | $5\times10^{-3}$ | $5\times10^{-5}$ | 1.5 | 10 | 11 |
| 2 | 2.36 | $3.36\times10^{-11}$ | $1.92\pi$ | | | | | |
| 3 | 2.72 | $1.36\times10^{-11}$ | $1.45\pi$ | | | | | |

The part surface altitude information of all scales is extracted from the multi-fractal surface by using the compactly supported wavelet of Daubechies, and the multi-resolution optimized multi-scale information is imported into CAD system. Figure 6 shows the ultimate multi-scale solid models of part surface topography. For the purpose of showing the surfaces of the multi-scale models more clearly, the surface altitude difference is enlarged by 4 times in Figures 6(a), (c) and (d), and 40 times in Figure 6(b), whose sampling length is 40mm extraordinarily.

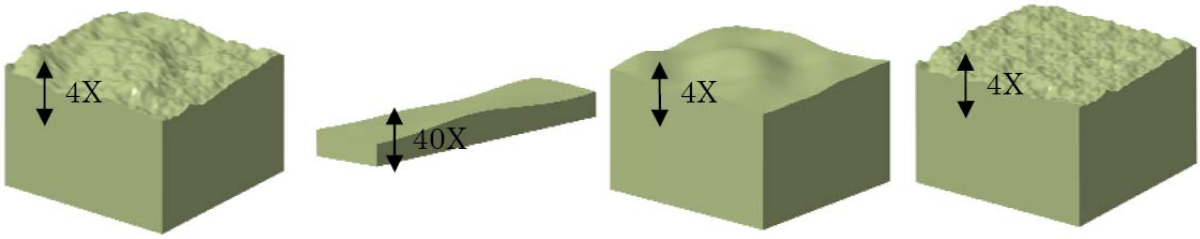


(a) Practical profile (b) Form error profile (c) Waviness profile (d) Roughness profile

FIGURE 6. Multi-scale solid models of part surface topography

5.2. **Contact analysis of part surface at the scale of roughness.** Because the elastic-plastic deformation of part surface is caused by micro-bulges of the surface in all shapes and sizes, the roughness profile of the multi-scale model is needed for the contact analysis of part surface. Considering computational complexity, the 1mm×1mm area of the roughness model is imported into Ansys12.0 to carry out the finite element analysis. In this paper, it is supposed that the contact objects are a flexible rough surface and a stiff flat surface. The element type is defined as SOLID186, and the elastic modulus and the Poisson ratio of the material are defined afterwards. The contact faces are the upper surface of the flexible body and the lower surface of the rigid body, so they should be generated with more elements extraordinarily. The finite element model for the contact analysis of part surface is built as shown in Figure 7, including 30424 nodes and 22550 elements.

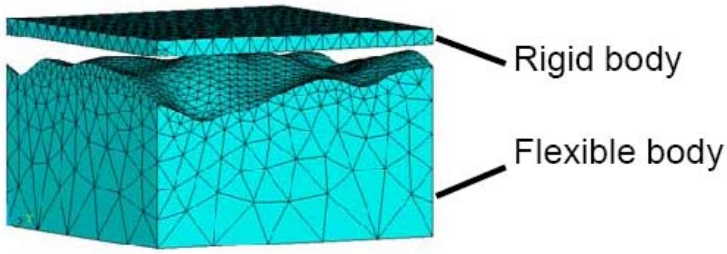


FIGURE 7. Finite element model for the contact analysis of part surface

The lower surface of rigid body is defined as the area for target with the element type of TARGE170, and the upper surface of flexible body is defined as the area for contact with the element type of CONTA174, and then the three-dimensional contact pair is created. The boundary condition on the flexible body and the rigid body is defined afterwards, and a downward load is applied on the upper surface of the rigid body, so that the rough surface deforms owing to the close contact of the two bodies. Figures 8 and 9 show the solution result of the finite element analysis. It indicates that some areas of the part surface are already at the stage of elastic deformation, while others are still at the stage of elastic deformation. Figure 10 shows the curve of the vertical displacement of the part surface with the change of the force in the whole contact process.

5.3. **Assembly quality analysis using virtual prototype of the machine tool at the scale of form error.** The effect of a part surface on assembly quality is principally the restriction of form error towards fitting property and fitting accuracy, since it changes effective magnitude of interference and effective magnitude of clearance between parts. In the product assembly analysis, however, it always considers the dimension error, but pays not enough attention to form error and position error of part surface, and the analysis

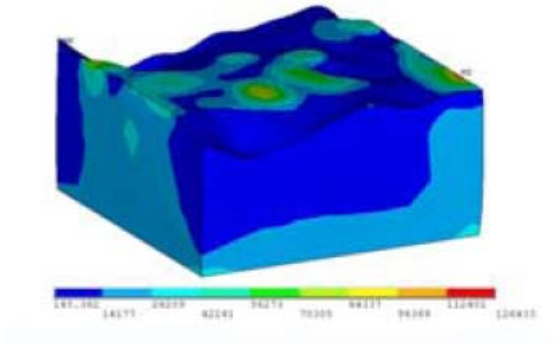

FIGURE 8. Equivalent stress of the flexible body

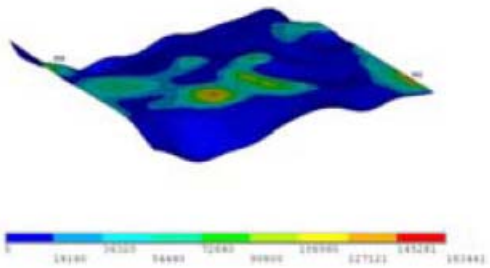

FIGURE 9. Pressure distribution of the part surface

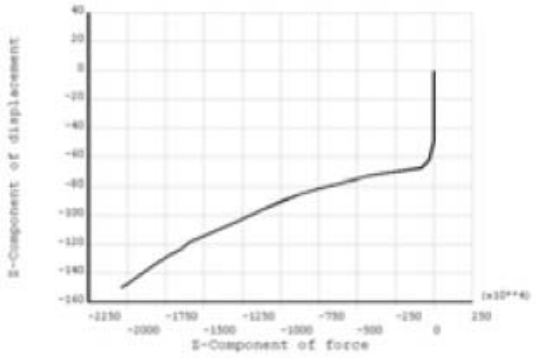


FIGURE 10. The curve of vertical displacement with the change of force

result is hard to meet the assembling requirement in the practical assembly. In our work, the virtual assembly using the multi-scale model of part surface topography is carried out, and the fitting accuracy after assembly is analyzed.

The subject investigated is still the guide rail of the gem processing machine tool, whose full size model is built including form error on its lower surface. It is calculated that the distance between two planes, which just contain the whole form error profile, is $\Delta = 18.43\mu m$. According to GB/T 1184-1996, it is at 5-grade in the flatness tolerance, and meets the design requirement of the gem processing machine tool. In virtual assembly, the guide rail and its adjacent parts can be treated as rigid bodies, because the load applied on the guide rail cannot cause sufficient contact, and it cannot lead to deformation at the scale of form error during the assembly operation.

The virtual assembly of the machine tool is carried out by controlling the assembly sequence and the assembly path of each part. Figure 11 shows the assembly operation of fixing the guide rail, which contains form error, to the beam of the machine tool. When the virtual assembly is completed, three sections of the assembly are cut perpendicularly to the longitudinal direction of the guide rail, and some partial details of the sections are enlarged by 4 times as shown in Figure 12. The effective magnitude of clearance of these sections is calculated, and the evaluation result of the fitting accuracy is obtained as shown in Figure 13, in which the maximum magnitude of clearance is $S_{\max} = 11.14\mu$m.

6. **Conclusions.** Nowadays, more and more attention has been paid to the effect of part surface quality on the product performances. A multi-scale based unified modeling method of part surface topography is proposed in this paper. The conclusions are as follows.

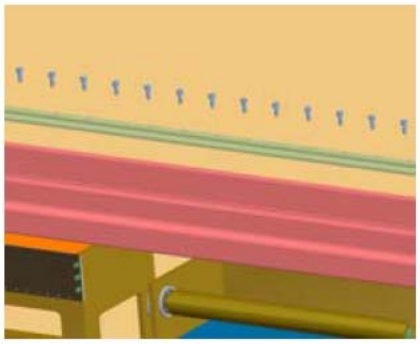

FIGURE 11. Virtual assembly of the guide rail

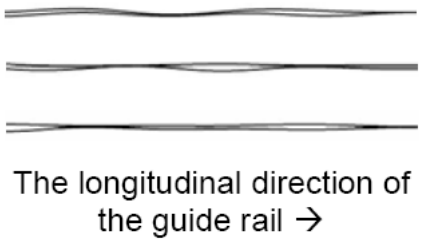


FIGURE 12. Partial sections of the guide rail and the beam

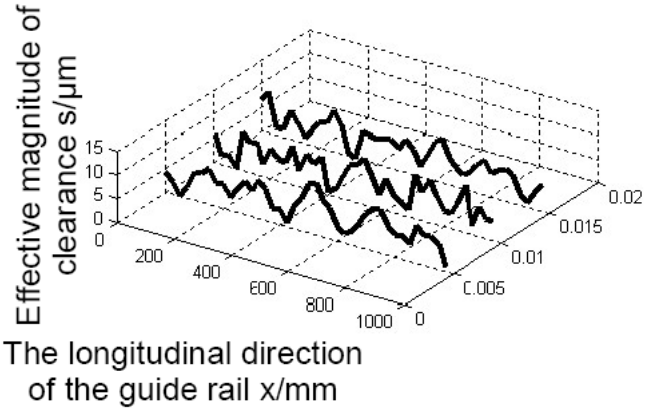


FIGURE 13. Calculation results of the fitting accuracy of the guide rail

1. The three-dimensional multi-fractal rough surface is well simulated according to three-dimensional multi-fractal characteristic function which is generalized in this paper. The micro-topography information of PSAF is decomposed into different scales by the multi-scale information extraction method based on wavelet analysis, so that various kinds of errors can be separated.
2. The storage space of the multi-scale model is saved and the computational efficiency is obviously improved by multi-resolution optimization proposed in this paper. The consistency between two surface profiles is verified by the part surface consistency evaluation method based on *PSMI* which is proposed in this paper. The information transmission model of multi-scale part surface reveals the process of information transmission and coupling in the life cycle of part surface.
3. The multi-scale unified model of the guide rail which is built in this paper meets the demands of various performance simulations, which can be used as the reference for structural design and technological selection of the gem processing machine tool. The multi-scale based unified modeling method of part surface topography proposed in this paper is applicable to describe the part with horizontal rough surfaces, and it needs to be studied further that how to describe and build the multi-scale model of a part with curved rough surfaces comprehensively, such as impeller blade and bearing roller.

**Acknowledgment.** The support of Project of NSFC (51075357, 50875239, 51005199) and Project of National Basic Research 973 Program of China (2011CB706503) and Fundamental Research Funds for the Central Universities (2010QNA4026) in carrying out this research is acknowledged.

## REFERENCES

[1] P. Dobrzanski and P. Pawlus, Digital filtering of surface topography: Part I. Separation of one-process surface roughness and waviness by Gaussian convolution, Gaussian regression and spline filters, *Precision Engineering*, vol.34, pp.651-658, 2010.

[2] W. E. Wilson, S. V. Angadi and R. L. Jackson, Surface separation and contact resistance considering sinusoidal elastic-plastic multi-scale rough surface contact, *Wear*, vol.268, pp.190-201, 2010.

[3] W. Grzesik and S. Brol, Wavelet and fractal approach to surface roughness characterization after finish turning of different workpiece materials, *Journal of Materials Processing Technology*, vol.209, pp.2522-2531, 2009.

[4] H. Zhang, Y. B. Yuan and F. Zhang, Engineering surface roughness filtering by B-spline, *Nanotechnology and Precision Engineering*, vol.7, no.6, pp.490-495, 2009.

[5] Q. H. Chen and Z. Li, Method of wavelet for picking up surface roughness, *Chinese Journal of Mechanical Engineering*, vol.35, no.3, pp.41-43, 1999.

[6] S. F. Lu and Z. Li, Composite characterization of fractal engineering surfaces, *Chinese Journal of Mechanical Engineering*, vol.38, no.8, pp.64-67, 2002.

[7] J. W. Hu, *A Study on Applications of Multi-Scale Estimation Theory to Engineering Surface Evaluation*, Master Thesis, Wuhan University of Technology, Wuhan, 2003.

[8] A. Majumdar and C. L. Tien, Fractal characterization and simulation of rough surfaces, *Wear*, vol.136, no.2, pp.313-317, 1990.

[9] A. Majumdar and B. Bhushan, Fractal model of elastic-plastic contact between rough surfaces, *Journal of Tribology*, vol.113, pp.1-11, 1991.

[10] M. Ausloos and D. H. Berman, A multivariate Weierstrass-Mandelbrot function, *Proc. of the Royal Society of London Series A*, vol.400, pp.331-350, 1985.

[11] K. Komvopoulos, Effects of multi-scale roughness and frictional heating on solid body contact deformation, *Comptes Randus Mecanique*, vol.336, pp.149-162, 2008.

[12] B. Bhushan and A. Majumdar, Elastic-plastic contact model for bi-fractal surfaces, *Wear*, vol.153, pp.53-64, 1992.

[13] L. Dong and Y. X. Zhang, Research on mathematical expression and simulation of multi-fractal profiles and surface, *Lubrication Engineering*, vol.4, pp.103-105, 2005.

[14] S. R. Ge and K. Tonder, The fractal behavior and fractal characterization of rough surfaces, *Tribology*, vol.17, no.1, pp.73-80, 1997.

[15] C. Wei and S. Jiang, Small target detection in flir imagery using multi-scale morphological filter and kernel density estimation, *International Journal of Innovative Computing, Information and Control*, vol.5, no.7, pp.1811-1817, 2009.

[16] S. Li, L. Peng and M. Zhao, Wavelet-based fast image inpainting for large scale missing regions, *International Journal of Innovative Computing, Information and Control*, vol.6, no.7, pp.3081-3091, 2010.

[17] Y. Xing, X. Wu and Z. Xu, Multiclass least squares auto-correlation wavelet support vector machines, *ICIC Express Letters*, vol.2, no.4, pp.345-350, 2008.

[18] Z. Zhang, Y. Ohara, H. Toda, T. Miyake and T. Imamura, De-noising method by combining adaptive line enhancer and complex discrete wavelet transform, *ICIC Express Letters*, vol.1, no.2, pp.145-151, 2007.

[19] Z. Zhang, T. Miyake and T. Imamura, Blind source separation by combining independent component analysis with the complex discrete wavelet transform, *International Journal of Innovative Computing, Information and Control*, vol.6, no.9, pp.4157-4172, 2010.

[20] C. Studholme, D. L. G. Hill and D. J. Hawkes, An overlap invariant entropy measure of 3D medical image alignment, *Pattern Recognition*, vol.32, pp.71-86, 1999.